RESEARCH ARTICLE

EFFECT OF STRUCTURAL HETEROGENEITY OF α-SYNUCLEIN MUTANTS ON THE AGGREGATION PROPENSITY

[1]Airy Sanjeev and *,[2]Venkata Satish Kumar Mattaparthi

[1]Molecular Modelling and Simulation Laboratory
[2]Department of Molecular Biology and Biotechnology, Tezpur University, Tezpur-784 028, Assam, India

ARTICLE INFO	ABSTRACT
	Parkinson's disease is related to the aggregation of α-synuclein but the effect of single-point mutations (A53T, E46K and A30P) on the early events of aggregation remains elusive. The effect of structural heterogeneity of α-synuclein mutants in promoting the dimerization is critical. From the conformational dynamics of monomers of α-synuclein (WT and mutants), we noticed mutants to display beta structures and more intra-molecular contacts. We also studied inter-molecular interactions promoting the dimerization. We observed lesser number of inter-molecular interactions in the homo-dimer of WT than the mutants. The interactions demonstrated here may be used to design potential inhibitors to inhibit dimerization.

Citation: Airy Sanjeev and Venkata Satish Kumar Mattaparthi, 2017. "Effect of structural heterogeneity of α-synuclein mutants on the aggregation propensity", *International Journal of Current Research*, 9, (07), 53448-53456.

INTRODUCTION

α-Synuclein (α-Syn)is an intrinsically disordered protein that aggregates into intra-cellular Lewy bodies (LB) and Lewy neuritis which are considered to be the pathological hallmarks for the occurrence of Parkinson's Disease(PD) (Spillantini *et al.*, 1997), a neuro-degenerative disorder. α-Syn is a micelle bound protein with 140 amino acids conserved in the vertebrates and expressed in the pre-synaptic nerve terminals in several regions of the brain (Bisaglia, Mammi and Bubacco, 2009). The insights into the α-syn plasticity and misfolding from differential micelle binding have been studied very recently (Mazumder, Suk and Ulmer, 2013). This unstructured protein binds to curved synaptic vesicle membranes in helical conformations but it misfolds into amyloid fibrils via β-sheet interactions (Lavedan, 1998). α-Syn basically comes from the synuclein family inherited from three highly expressed genes that are SNCA, SNCB and SNCG of α, β and γ synuclein respectively (Lavedan, 1998). The aggregation propensity of α-syn is still not understood though various genetic data have supported the pathological role of this protein (Lashuel, Overk, Oueslati, Masliah, 2013). The cause for the familial Parkinsonism and the fibrillation propensity is due to the multiplication of the gene that encodes α-syn protein called the SNCA gene (Chartier-Harlin, *et al.*, 2004) and also for the

occurrence of point mutation that enhances the Parkinsonism. A53T, A30P and E46K (Kruger *et al.*, 1998; Polymeropoulos *et al.*, 1997 and Zarranz *et al.*, 2004) are the well-known point mutations located in the N-terminal region of α-syn protein (Figure 1). These mutation results in the conversion of one amino acid to another and for this reason the early onset of PD initiates. As α-syn helps in the formation of LB, the aggregation propensity is a key factor for the pathogenesis of PD (Coskuner and Wise-Scira, 2013). Recently it has been observed that the α-syn monomers and oligomers are neurotoxic in nature (Outeiro *et al.*, 2008; Winner *et al.*, 2011). The aggregation mechanism of α-syn protein is basically due to the disordered structures of the monomeric and oligomeric units (Li, Uversky and Fink, 2001; Li, Uversky and Fink, 2002). A53T mutant present in α-syn has been shown to alter the neurotoxicity and aggregation of the wild type (WT) α-syn protein. Different trends in the neurotoxicity of the WT and A53T mutant-type α-syn proteins have been reported in the recent literature (Choong and Say, 2011) in which the A53T mutant-type α-syn has been reported to be neurotoxic andWT α-syn as neuroprotective toward the SH-SY5Y cells in the presence of rotenone and maneb. Several studies have highlighted a straight filament structure for the WT α-synand twisted structure for A53T mutant (Choi *et al.*, 2004; Conway, Harper and Lansbury, 1998; Giasson, Uryu, Trojanowski and Lee, 1999).The increased aggregation rate of A53T mutant has been observed in various studies (Choi *et al.*, 2004; Conway, Harper and Lansbury, 1998; Conway *et al.*, 2000; Giasson,

*Corresponding author: **Venkata Satish Kumar Mattaparthi,**
Department of Molecular Biology and Biotechnology, Tezpur University, Tezpur-784 028, Assam, India.

Uryu, Trojanowski and Lee, 1999; Kamiyoshihara, Kojima, Ueda, Tashiro, and Shimotakahara, 2007; Lashuel *et al.*, 2002; Li, Uversky and Fink, 2001; Li, Uversky and Fink, 2002; Narhi *et al.*, 1999; Ono, Ikeda, Takasaki and Yamada, 2011; Serpell, Berriman, Jakes, Goedert, and Crowther, 2000) by which the idea of β-rich content can be supported. However, A30P does not influence the effect of phosphorylation on the formation of inclusions (Smith *et al.*, 2005). But in another *in vitro* study (Ishii *et al.*, 2007) it has been reported that phosphorylation of α-syn by casein kinase 2 (CK2) is comparatively slower for the mutants (A30P and A53T) than the WT α-syn. From the literature (Mbefo *et al.*, 2015) it was observed that enhanced phosphorylation of the E46K mutant could be linked to its aberrant subcellular localization. E46K mutant also found to exhibit enhanced S129 phosphorylation in mammalian cell lines and in yeast (Mbefo *et al.*, 2015). So the effect of pathogenic single point mutations in α-synon the early events of aggregation remains elusive.

In this study, we have focused on the two important objectives:

1) Conformational dynamics of monomers of mutants and WT α-syn using molecular dynamics (MD) simulation,
2) The effect of structural heterogeneity of α-syn mutants in promoting the dimerization process. As dimer formation is the important and initial step for the accumulation of LB, we investigated the intra-molecular interactions in the dimer using PDBSum online server (Laskowski, 2001). By performing *in silico* study on the WT and mutants of α-syn, we can get an insight into the aggregation propensity and also various inhibiting factors that can further improve drugs and therapeutics in the upcoming era.

MATERIALS AND METHODS

Molecular Dynamics simulation of WT and mutants of α-Syn

The initial micelle bound 3D structure of the WT (*1XQ8*) of α-syn was taken from Protein Data Bank (Berman *et al.*, 2000). The 3D structures of mutants of α-syn (A30P, A53T and E46K) were constructed from WT structure by replacing the respective amino acid with the appropriate one using Swiss-PDB viewer software (Guex and Peitsch, 1997). In order to comparethe conformational dynamics of the mutants with respect to WT α-syn, we carried out MD simulation using AMBER12 software package (Case *et al.*, 2012) and ff99SB (Hornak *et al.*, 2006) force field. The topology and co-ordinate files required for MD simulation were generated using LEaP module of AMBER package. The negative charges in the monomers of WT and mutants were neutralized by appropriate number of sodium ions. The WT and variants of α-syn were then minimized in two stages for ensuring the stability of the structure;first it was subjected to 500 steps of steepest decent minimization followed by another 500 steps conjugate gradient. Then the conformers were constrained by 50 kcal/mol/Å^2 harmonic potential to remove the unfavorable contacts. As a whole, the systems (monomer along with water and sodium ions) were subsequently minimized using 1,000 steps of steepest decent minimization in the absence of harmonic restraints. The conformers were then heated gradually from 0 to 300 K over a timescale of 20 ps under atomic restraints. After heating, equilibration dynamics was

performed for 100 ps. To ensure equilibration for the system, Root Mean Square Deviation (RMSD), potential, kinetic and total energy, pressure, density and temperature for the variants of α-syn and WT were monitored. To constrain all the bonds, the shake algorithm (Ryckaert, Ciccotti and Berendsen, 1977) was used and the time step of the simulation was 2 fs. Following this, the system was simulated for a last step of 100 ps long MD in the isothermal-isobaric ensemble. Berendsen thermostat (Berendsen *et al.*, 1984) was used for temperature control. Setting the pressure and temperature of the simulations to 1 barand 300 K, production run was carried out for 100 ns in NPT to collect the trajectories and generate the data. For visualization of the trajectories, VMD package (Humphrey, Dalke and Schulten, 1996) was used after every MD run.

Construction of homo-dimers of WT and mutants (A30P, A53T and E46K) of α-syn

To study the inter-molecular interactions between the monomeric units in the dimers of mutants (A30P, A53T, and E46K) and WT, the conformer representing the most populated clusters after equilibration was used to construct the dimeric structures. Using PatchDock (Duhovny, Nussinoy and Wolfson, 2002) server, the selected conformer was docked to the copy of itself, and the best dimer conformer was selected based on maximum contact surface area and minimum free energy. PatchDock works by the principle of geometric–based docking algorithm (Zhang, Vasmatzis, Cornette and DeLisi, 1997) that selects the optimum candidate solution with the RMSD clustering to remove the redundant models. The selected model was then given a score that implies docking transformation of one of the monomer with other monomer which optimally fit inducing both small amounts of steric clashes and wide interface areas. In our study, we used a default RMSD value of 4 Å. The dimer complex with the maximum surface area and minimum atomic contact energy was selected.

Inter-molecular Interactions in the dimmers

We then analyzed the inter-molecular interactions between the monomeric units of dimer of WT and mutants using PDBSum online server (Laskowski, 2001).The server gives a brief description about the interfaces between the chains, interacting interface, interactions across any selected interface of the dimer complex and overview of which chains interact with the other chain. The best dimer conformer obtained from Patch Dock based on surface shape complementarity score, geometric surface area, atomic contact energy (ACE) was submitted onto the PDBSum server. The summary of the interacting residues, bonded and non-bonded contacts involved between the monomeric units in the dimer of WT and mutants were then obtained from PDBSum.

RESULTS AND DISCUSSION

Conformational dynamics of monomers of mutants and WT α-syn using molecular dynamics (MD) simulation

To study the effect of mutants on the aggregation propensity of α-syn, we have comparedthe conformational dynamics of WT and its primary mutants (A30P, A53T and E46K) using all atom molecular dynamics (MD) simulation.

Root Mean Square Deviation (RMSD) of the mutants and WT

The degree of conformational changes for the WT α-syn and the mutants during the time course of simulation was monitored by the Cα root mean square deviation. The backbone RMSD values of structures of the WT and mutants relative to their corresponding initial reference structure have been calculated and represented in Figure 2. The RMSDs for the three mutants (A53T, A30P and E46K) and WT using the backbone atoms of each conformer settles between 25-30 Å and hence the structure of the conformers is well maintained throughout the simulation run (100 ns). However the N-terminal ends of the mutant experiences slightly higher fluctuation than the NAC (*non-amyloid β-component*) domain and C-terminal regions. As α-syn belongs to an intrinsically disordered protein, we observed a sudden deviation in the RMSD value from 10 Å to 40 Å for the mutants and WT respectively. Thus we can see that the aggregation propensity increases for the mutants when compared to the WT α-syn as the RMSD value for the mutants fluctuates more when compared to WT α-syn.

Radius of Gyration (Rg) for the mutants and WT

For the WT and mutants of α-syn, we also measured the radius of gyration which is an indicator of protein structure compactness (Lobanoy, Bogatyreva and Galzitskaya, 2008). We observed A30P and A53T structures present a higher probability for structures with Rg values varying between 45 and 50 Å. While WT and E46K structures present higher probability for structures with Rg values varying between 45 and 48 Å (Figure 3). We thus see a decrease in long range interactions in the structure of the WT and E46K mutant type α-syn rather than the A30P and A53T α-syn protein. We also note that the Rg values of the WT α-syn agree with the range of Rg values reported by previous theoretical studies (Coskuner, and Wise-Scira, 2013; Losasso, Pietropaolo, Zannoni, Gustincich and Carloni, 2011).

B-factor Analysis

To analyze the local deformability for the C-α atom in WT and the mutants of α-syn we analyzed B factor. B-factors give information about the spatial fluctuations of atoms around their equilibrium position. The B-factor values obtained for the backbone C-α atom in WT and mutants of α-syn were calculated from the corresponding MD simulation trajectories and were plotted against their residue numbers (Figure 4). From these plots we can see that in the case of the WT, C-α atoms of the residues in the region between 70-100 and 120-130 shows more flexibility than the residues in the other regions while in the case of mutants we observed that C-α atom of residues in the region between 50-100 and in between 125-130 show more flexibility. Among the three mutants structure of α-syn, we observed high atomic fluctuations in E46K both in the N-terminal and C-terminal regions.

Secondary Structure Analysis for the mutants and WT of α-Syn

Using the Kabsch and Sander algorithm incorporated in their DSSP (Dictionary of Secondary Structure for Protein) program (Kabsch and Sander, 1983) the secondary structure analysis was carried out for the WT protein and the mutants of α-syn.

The results for the secondary structure analysis are plotted in Figure S1.

The plot shows the secondary structural variation of each residue as a function of simulation time period. In the case of mutants, we see anti-parallel β sheets near the C-terminal (residue index: 120-140) and parallel β sheets near the N-terminal regions (residue index: 25and 39). In the other regions of the mutants we observed secondary structure transitions from 3_{10} helix and α-helix to turns. In the case of WT; we observe the regions near the N-terminal (residue index: 25and 35) and C-terminal regions to have anti-parallel β sheets (residue index: 115,117,118,123,125), and parallel β sheets near the N-terminal regions. In the other regions of WT, we observed many of the residues showing secondary structure transitions from helix to turns. And among those mutants, A53T was seen to have a higher helical content in comparison to other variants. So the existence and rapid changes in structural dynamics of WT and mutants is clearly visible from secondary structure analysis. Therefore we suggest that monomeric units in the stable homo-dimer can have helical as well as β-structured forms.

Apart from that, we also calculated the percentage of individual secondary structure content in WT and mutants across all conformations using YASARA software (Kreiger, Koraimann and Vriend, 2002) sampled during the production job of trajectories and the results are discussed in Table 1. From the Table 1, we observed that WT α-syn contain higher amount of α-helix than the mutants. Thus we can conclude that the mutants possess the ability to fibrillate more when compared to the WT α-syn. We also quantified the probable secondary structures that each residue can adopt in the case of WT and mutants of α-syn (see Figure S2). From Figure S2, we noticed the probability score of secondary structure assignment per residue present in WT and mutants. We observed WT to have a higher helical content than mutants of α-syn.

Contact Map Analysis

In WT and mutants of α-syn we investigated the intra-molecular contacts present between the N-terminal and NAC domain regions using CMA (Contact Map Analysis), one of the application program of the online software SPACE (Structure Prediction and Analysis based on Complementarity with Environment) (Sobolev *et al.*, 2005). This program allows to analyze contacts between two chains or within one chain in a given PDB file based on shape and chemical complementarity. To investigate the residue-residue contacts between the N-terminal and NAC domain regions of WT and mutants, a contact area of threshold above 8 Å² has been considered for the analysis. The contact map analysis for the WT and mutants are shown in Figure 5. Contact map analysis for WT and mutants shows the highest trend in A30P with eight residues interacting with each other in N-terminal and NAC domain that share a contact area greater than the threshold that we considered for the analysis. This is in agreement with the inferences that have been obtained from Radius of gyration analysis (Figure 3). Only four residues of N-terminal and NAC domain are observed to share a contact area greater than the threshold value of 8 Å² limit in A53T mutant of α-syn. The contact map analysis therefore supports varied intra-molecular interactions between the N-terminal and NAC domain regions in WT and mutants of α-syn.
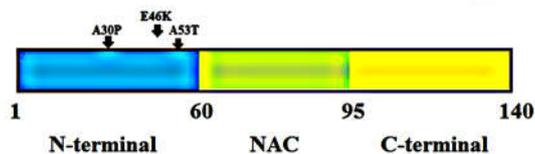
Figure 1. Schematic representation of the position of primary mutants in the α-synuclein protein
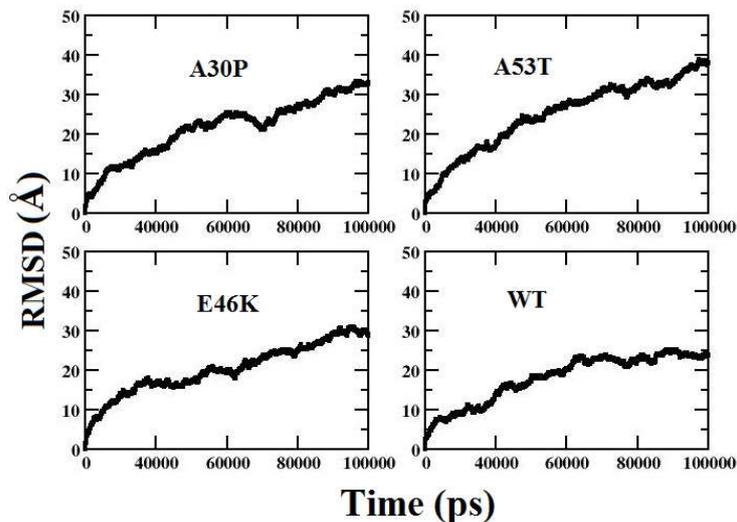

Figure 2. RMSD plot for the WT and mutants of α-synuclein protein as a function of simulation time-period
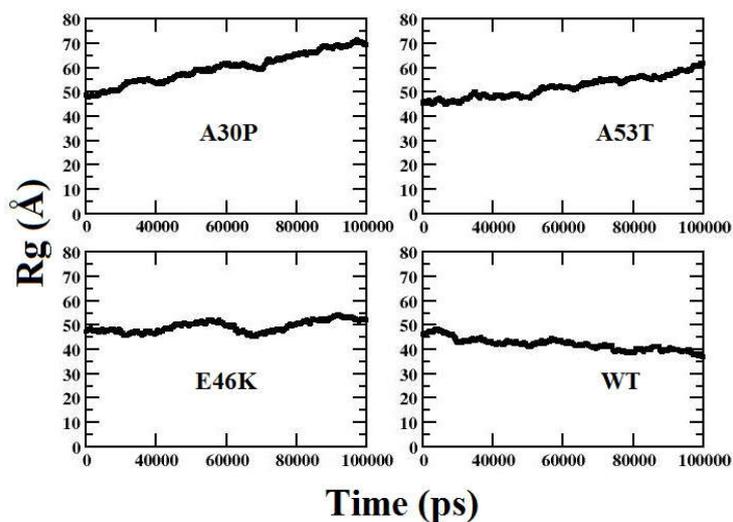

Figure 3. Rg plot for the WT and mutants of α-synuclein protein as a function of simulation time-period
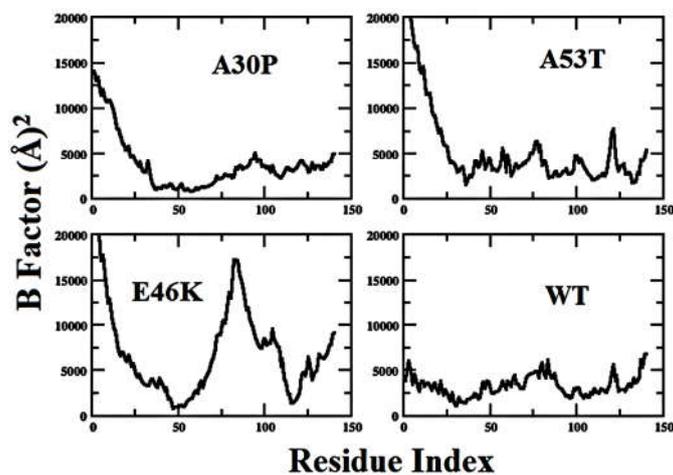

Figure 4. B-factor plot for the WT and mutants of α-synuclein protein as a function of residue index
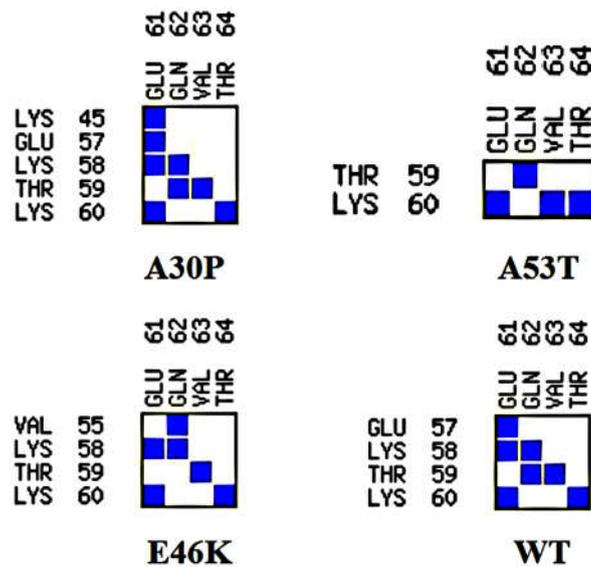
Figure 5. Contact Map Analysis plot of the WT and mutants of α-synuclein between the N-terminal and NAC domain
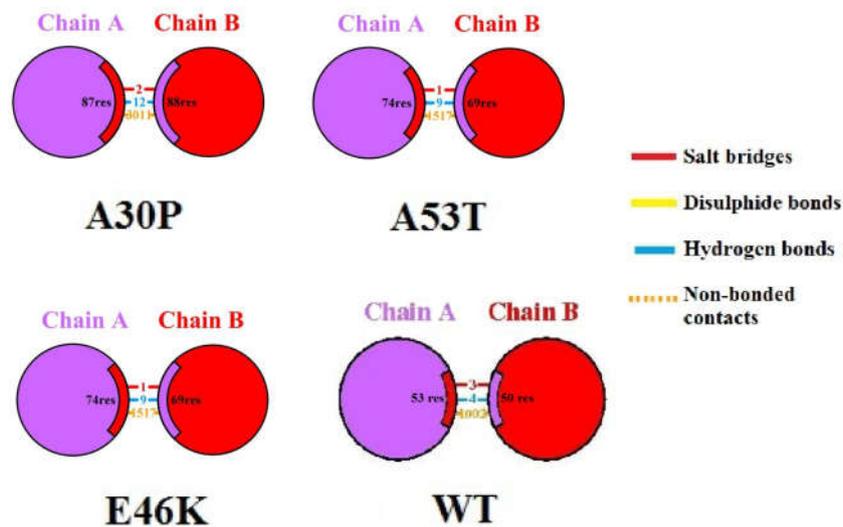

Figure 6. Interface statistics for dimer conformers of A30P, A53T, E46K and WT obtained showing hydrogen bonds, salt-bridge, non-bonded contacts and disulfide bonds from PDBSum server

Table 1. Secondary Structure content of the WT protein and mutants of α-synuclein showing the secondary contents of α- helix, β-sheets, Turns, 310 –helix and Coils

α-Synuclein Variants	Secondary Structure content				
	α- helix (%)	β-sheets (%)	Turns (%)	3_{10} –helix (%)	Coils (%)
A30P	19.3	0	28.6	0	52.1
A53T	17.1	1.4	22.9	0	58.6
E46K	9.3	0	28.6	0	62.1
WT	13.6	0	28.6	0	57.9

Table 2. Interface plot statistics of the mutants and WT showing the total number of interface residues, interface area, number of hydrogen bonds, number of salt bridge and total non-bonded contacts

Dimer	Chain	No. of interface residues	Interface area (Å²)	No. of salt bridges	No. of disulphide bonds	No. of hydrogen bonds	No. of Non-bonded contacts
	A	87	4020				
A30P	*B*	88	4057	2	-	12	3011
	A	74	3381				
A53T	*B*	69	3572				
				1	-	9	1517
	A	74	3403				
E46K	*B*	69	3592				
				1	-	9	1517
	A	53	2238				
WT	*B*	50	2241	3	-	4	1002

The effect of structural heterogeneity of α-syn mutants in promoting the dimerization process

Inter-molecular interactions in homo-dimers of WT and mutants of α-syn

In order to study the inter-molecular interactions between the monomeric units in the corresponding homo-dimer of the mutants and WT α-syn, we prepared dimer complex structures from PatchDock. Using the PatchDock online server, the best docked homo-dimer complex structure for the mutants and WT α-syn was selected based on atomic contact energy value, interface area and geometric shape complementary score (Figure S3). We noticed that in case of A30P homo-dimer, the monomeric units interact with each other with a geometric shape complementarity score of 21108, approximate interface area of 5915.80 $Å^2$ and atomic contact energy (ACE) of -639.72 kcal/mol. In A53T homo-dimer complex, we observed the monomeric units interact with each other with a geometric score of 23412, approximate interface area of 4261.20 $Å^2$ and atomic contact energy (ACE) of -409.53 kcal/mol. And in E46K homo-dimer complex, we noticed the inter-monomeric interaction with a geometric score of 24016, approximate interface area of 4276.20 $Å^2$ and atomic contact energy (ACE) of -407.24 kcal/mol. However, for WT α-syn homo-dimer, we observed the inter-monomeric interaction with geometric score of 14454, approximate interface area of 3312.90 $Å^2$ and atomic contact energy (ACE) of -365.18 kcal/mol. We also then analyzed the interacting residues in the best docked homo-dimer complex structure for the mutants and WT α-syn using PDBSum online server. The various inter-molecular interactions between the monomeric units of WT and mutants of α-syn are shown in Figure 6. The results for the interface statistics are summarized in Table 2. From Table 2, we can see the total number of interface residues in the homo-dimer complex for mutant A30P was found to be 175 and the interface area for each monomeric unit involved in the interaction was observed to be more than 4020 $Å^2$. While in the case of WT we observed the total number of interface residues to be 103 and the interface area to be more than 2238 $Å^2$. We see the stable homo-dimer of mutants and WT were stabilized by molecular interactions like hydrogen bonding and non-bonded contacts. In one of the recent study it has been suggested that stable dimers could be formed from helical as well as β-structured forms of the monomer (Mane and Stepanova, 2016). From Table 2, it can be seen that the number of hydrogen bonds and non-bonded contacts to be more in the case of mutants (*A30P, A53T and E46K*) when compared to WT α-syn. This again suggests that the mutants can undergo aggregation at a faster rate when compared to the WT α-syn. We also noticed the central hydrophobic region of the α-syn monomer plays a prominent role in all dimer structures suggesting that hydrophobic interactions play an important role in the binding affinity as observed in one of the earlier study (Sahu, Woodside and Tuszynski, 2015). In one of the recent study it has been shown that single-point mutations in α-syn promote dimerization, and the structural heterogeneity of α-syn dimers could lead to different aggregation pathways (Ly *et al.*, 2015).

Conclusion

In this study we demonstrate the effect of structural heterogeneity of α-syn mutants in promoting the early events of the aggregation process in particular the dimerization

process. From the conformational dynamics analysis of the monomers of α-syn(WT and mutants), we noticed the mutants (A30P and A53T) to display extended beta structures and to have more number of intra-molecular contacts between N-terminal and NAC domain. We also characterized the salient inter-molecular interactions between monomeric units in homo-dimers of the α-syn(WT and mutants).We found relatively lesser number of inter-molecular interactions in the homo-dimer of WT than the mutants. Our findings in this study also suggest the monomeric units in the stable homo-dimer to have helical as well as β-structured forms. As a whole we see the mutants of α-syn are more likely to aggregate than WT. The various interactions investigated in this study can be used to design potential inhibitors to control the early events of α-syn aggregation.

Conflict of Interest

The author(s) confirm that this article content has no conflict of interest.

Abbreviation

α-Syn, α-Synuclein; MD, Molecular Dynamics; WT, Wild Type; ACE, Atomic Contact Energy; LB, Lewy Bodies; PD, Parkinson's Disease; CK2, Caesin kinase 2; RMSD, Root Mean Square Deviation; Rg, Radius of Gyration; DSSP, Dictionary of Secondary Structure of Proteins; CMA, Contact Map Analysis; SPACE, Structure Prediction and Analysis based on Complementarity with Environment; NAC, Non-amyloid β component

REFERENCES

Berendsen, H.J. C., Postma, J.P.M., Van Gunsteren, W.F., DiNola, A. and Haak, J.R., 1984. Molecular dynamics with coupling to an external bath. *Journal of Chemical Physics,* 81, 3684-3690.

Berman, H.M., Westbrook, J., Feng, Z., Gilliland, G., Bhat, T.N., Weissig, H., Shindyalov, I.N. and Bourne1, P.E. 2000. The Protein data bank. *Nucleic Acids Research*, 28, 235-242.

Bisaglia, M., Mammi, S., and Bubacco, L., 2009. Structural in sights on physiological functions and pathological effects of alpha-synuclein. *FASEB Journal*, *23*, 329–340. doi: 10.1096/fj.08-119784

Case, D.A., Darden, T.A., Cheatham, III T.E., Simmerling, C.L., Wang, J., Duke, R.E., Luo, R., Walker, R.C., Zhang, W., Merz, K.M., Roberts, B., Hayik, S., Roitberg, A., Seabra, G., Swails, J., Gotz, A.W., Kolossvary, I., Wong, K.F., Paesani, F., Vanicek, J., Wolf, R.M., Liu, J., Wu, X., Brozell, S.R., Steinbrecher, T., Gohlke, H., Cai, Q., Ye, X., Wang, J., Hsieh, M. J., Cui, G., Roe, D.R., Mathews, D.H., Seetin, M.G., Salomon-Ferrer, R., Sagui, C., Babin, V., Luchko, T., Gusarov, S., Kovalenko, A., and

Kollman, P.A. 2012.AMBER 12, University of California, San Francisco.

Chartier-Harlin, M.C. *et al.* 2004. α-synuclein locus duplication as a cause of familial Parkinson's disease. *Lancet*, 364, 1167–1169.

Choi, Woong, Zibaee, Shahin, Jakes, Ross, Serpell, Louise, C., Davletov, Bazbek, Crowther, Anthony, R. and Michel,G. 2004. Mutation E46K increases phospholipid binding and assembly into filaments of human alpha-synuclein. *FEBS Letters*, 576 (3), 363-368.

Choong, C. J., and Say, Y. H. 2011. Neuroprotection of alphasynuclein under acute and chronic rotenone and maneb treatment is abolished by its familial Parkinson's disease mutations A30P, A53T and E46K. *Neurotoxicology*, 32, 857−863.

Conway, K. A., Harper, J. D., and Lansbury, P. T. 1998. Accelerated in vitro fibril formation by a mutant alpha-synuclein linked to early-onset Parkinson disease. *Nature Medicine*, 4, 1318−1320.

Conway, K. A.*et al.,* 2000. Acceleration of oligomerization, not fibrillization, is a shared property of both alpha-synuclein mutations linked to early-onset Parkinson's disease: Implications for pathogenesis and therapy. *Proceedings of the National Academy of Sciences, 97*(2):571-6.

Coskuner,O. and Wise-Scira,O. 2013. Structures and Free Energy Landscapes of the A53T Mutant-Type α‑Synuclein Protein and Impact of A53T Mutation on the Structures of the Wild-Type α‑Synuclein Protein with Dynamics, dx.doi.org/10.1021/cn400041j | *ACS Chemical Neuroscience*, 4, 1101−1113.

Duhovny, D., Nussinov, R., and Wolfson, H.J. 2002. Efficient unbound docking of rigid molecules, 185-200, Berlin Heidelberg: Springer-Verlag.

Giasson, B. I., Uryu, K., Trojanowski, J. Q., and Lee, V. M. Y. 1999. Mutant and wild type human alpha-synucleins assemble into elongated filaments with distinct morphologies in vitro. *Journal of Biological Chemistry*, 274, 7619−7622.

Guex, N., and Peitsch, M.C., 1997. SWISS-MODEL and the Swiss-pdb viewer: an environment for comparative protein modeling. *Electrophoresis,*18, 2714-2723.

Hornak, V., Abel, R., Okur, A., Strockbine, B., Roitberg, A. and Simmerling, C. 2006. Comparison of multiple Amber force fields and development of improved protein backbone parameters. *Proteins,*65, 712-725.

Humphrey, W., Dalke, A. andSchulten, K. 1996. VMD: visual molecular dynamics. *Journal of Molecular Graphics*, 14, 33–38.

Ishii, A. *et al.* 2007. Casein kinase 2 is the major enzyme in brain that phosphorylates Ser129 of human alpha-synuclein: Implication for alpha-synucleinopathies. *FEBS Letters*, 581, 4711-7.

Kabsch, W. and Sander, C. 1983. Dictionary of protein secondary structure: pattern recognition of hydrogen-bonded and geometrical features. *Biopolymers*, 22, 2577-2637.

Kamiyoshihara, T., Kojima, M., Ueda, K.,Tashiro, M. and Shimotakahara, S. 2007. Observation of multiple intermediates in alpha-synuclein fibril formation by singular value decomposition analysis. *Biochemical and Biophysical Research Communications, 355(2):*398-403

Krieger, E., Koraimann, G. and Vriend, G. 2002. Increasing the precision of comparative models with YASARA NOVA—a self-parameterizing force field. *Proteins,* 47,393-402.

Kruger, R.*et al.* 1998. Ala30Pro mutation in the gene encoding α-synuclein in Parkinson's disease. *Nature Genetics,* 18, 106–108.

Lashuel, H. A.*et al.,* 2002. Alpha-synuclein, especially the Parkinson's disease-associated mutants, forms pore-like annular and tubular protofibrils. *Journal of Molecular Biology*, 322, 1089–1102.

Lashuel, H.A., Overk, C.R., Oueslati, A. and Masliah, E. 2013.The many faces of α-synuclein: from structure and toxicity to therapeutic target. *Nature Reviews Neuroscience*, 14, 38-48.

Laskowski, R.A. 2001. PDBsum: summaries and analyses of PDB structures. *Nucleic Acids Research,* 29, 221-222.

Lavedan,C. 1998. The synucleinfamily. *Genome Research*, 8, 871–880.

Li, J., Uversky, V. N., and Fink, A. L. 2001.Effect of familial Parkinson's disease point mutations A30P and A53T on the structural properties, aggregation, and fibrillation of human alpha-synuclein .*Biochemistry*, 40, 11604−11613.

Li, J., Uversky, V. N., and Fink, A. L. 2002. Conformational behavior of human alpha-synuclein is modulated by familial Parkinson's disease point mutations A30P and A53T. *Neurotoxicology,* 23,553−567.

Lobanov, M.Y., Bogatyreva, N. S. andGalzitskaya, O. V. 2008. Radius of gyration as an indicator of protein structure compactness. *Molecular Biology*, 42, 623-628. doi: 10.1134/s0026893308040195

Losasso, V., Pietropaolo, A., Zannoni, C., Gustincich, S. and Carloni, P. 2011. Structural role of compensatory amino acid replacements in the α-synuclein protein. *Biochemistry*, 50, 6994-7001. Doi: 10.1021/bi2007564.

Lv, Z. *et al.* 2015. Direct Detection of a-Synuclein Dimerization Dynamics: Single-Molecule Fluorescence Analysis. *Biophysical Journal*, 108, 2038–2047.

Mane, J.Y. and Stepanova, M. 2016.Understanding the dynamics of monomeric, dimeric, and tetrameric a-synucle in structures in water. *FEBS Open Biology*, 6, 666–686.

Mazumder, P., Suk, J.E. and Ulmer, T.S. 2013. Insight into α-Synuclein Plasticity and Misfolding from Differential Micelle Binding. *Journal of Physical Chemistry B*, 117(39): 11448–11459. doi:10.1021/jp402589x.NIH

Mbefo, M.*et al.,* 2015.The Parkinson's Disease Mutant E46K Enhances Alpha-Synuclein Phosphorylation in Mammalian Cell-lines, in Yeast and In Vivo, *Journal of Biological Chemistry,*10,1074/jbc.M114.610774jbc.M114.610774.

Narhi, L.*et al.,* 1999. Both familial Parkinson's disease mutations accelerate alpha-synuclein aggregation. *Journal of Biological Chemistry,* 274, 9843–9846.

Ono, K., Ikeda, T., Takasaki, J. and Yamada, M., 2011. Familial Parkinson disease mutations influence alpha-synuclein assembly. *Neurobiology of Disease,* 43, 715–724.

Outeiro, T. F. *et al.* 2008.Formation of Toxic Oligomeric α-Synuclein Species in Living Cells. *Plos One*, 3, No. e1867.

Polymeropoulos, M.H. *et al.* 1997.Mutation in the α-synuclein gene identified in families with Parkinson's disease. *Science*, 276, 2045–2047.

Ryckaert, J.P., Ciccotti, G. and Berendsen, H.J.C., 1977. Numerical integration of the cartesian equations of motion of a system with constraints: molecular dynamics of n-alkanes. *Journal of Computational Physics,* 23, 327.

Sahu, K.K., Woodside, M.T. andTuszynski, J.A. 2015. α-Synuclein dimer structures found from computational simulations. *Biochimie.* Doi: 10.1016/j.biochi.2015.07.011.

Serpell, L. C., Berriman, J., Jakes, R., Goedert, M., and Crowther, R. A., 2000. Fiber diffraction of synthetic alpha-synuclein filaments shows amyloid-like cross-beta conformation. *Proceedings of the National Academy of Sciences, U. S.A.*, 97, 4897−4902.

Smith, W.W.*et al.,* 2005. Alpha-synuclein phosphorylation enhances eosinophilic cytoplasmic inclusion formation in SH-SY5Y cells. *Journal of Neuroscience,* 25, 5544-5552.

Sobolev, V. *et al.,* 2005. SPACE: a suite of tools for protein structure prediction and analysis based on complementarity and environment. *Nucleic Acids Research*, 33, 39-43.

Spillantini, M. G., Schmidt, M.L., Lee, V.M.Y., Trojanowski, J.Q., Jakes, R. and Goedert, M. 1997. Alpha-synuclein in Lewy bodies. *Nature*, *388*, 839–840

Winner, B.*et al.* 2011.In vivo demonstration that alphasynucleinoligomers are toxic.*Proceedings of the National Academy of Sciences,* U.S.A., 108, 4194−4199.

Zarranz, J.J. *et al.* 2004. The new mutation, E46K, of α-synuclein causes Parkinson and Lewy body dementia. *Annals of Neurology,* 55, 164–173.DOI: 10.1002/ana.10795

Zhang, C., Vasmatzis, G., Cornette, J.L., and DeLisi, C. 1997. Determination of atomic desolvation energies from the structures of crystallized proteins. *Journal of Molecular Biology,* 267, 707-726.
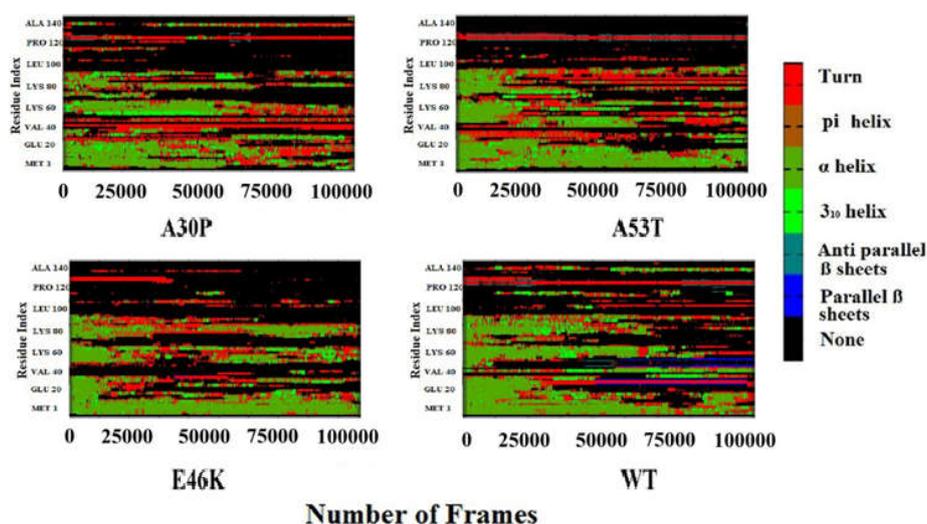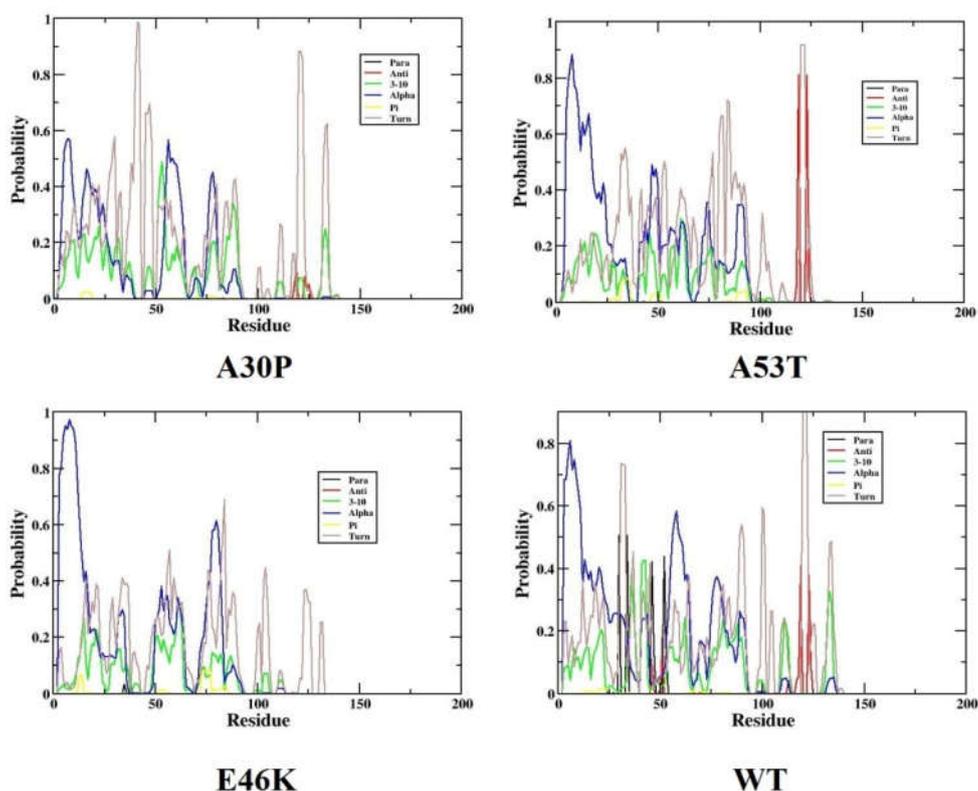
Supplementary Information

Figure S1: Secondary Structure of the WT and mutants of α-synuclein protein using DSSP plot

Figure S2: Probability Score of the mutants and WT as a function of residue index
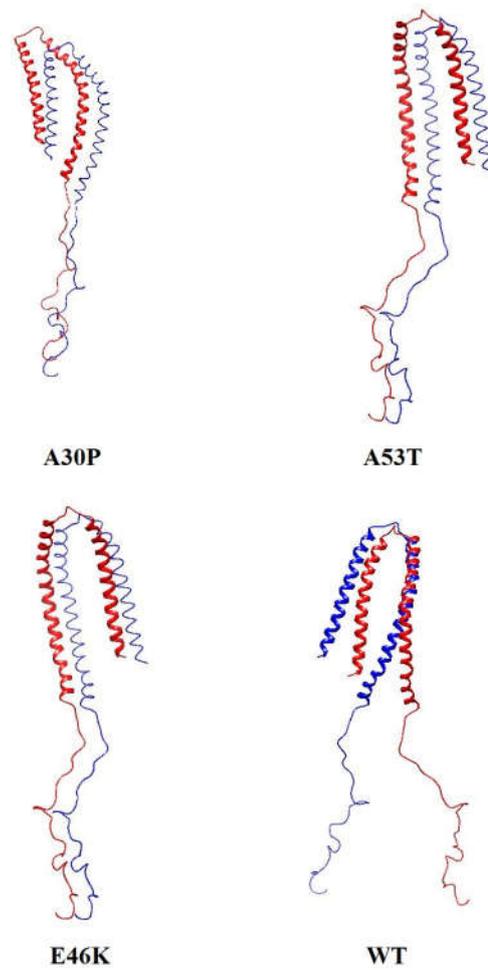
A30P

A53T

E46K

WT

Figure S3: **Dimer complex of the mutants and WT having the best atomic contact energy (ACE), geometrical shape complementarity score and surface area**

****